Universidad del País Vasco Euskal Herriko Unibertsitatea

MEDIKUNTZA ETA ERIZAINTZA FAKULTATEA
FACULTAD DE MEDICINA Y ENFERMERÍA

biocruces bizkaia
osasun ikerketa institutua
instituto de investigación sanitaria

Master's Thesis / Trabajo Fin de Master

Transcriptomic approach to identify biomarkers for primary progressive multiple sclerosis in populations of dendritic cells

Author:

Ainhoa Fiat Arriola

Director:

Iraide Alloza Moral

Director:

Mar Mendibe Bilbao

Date

September 16th, 2022

INDEX

1. ABSTRACT

Multiple sclerosis (MS) is an autoimmune disease of the central nervous system (CNS) characterized by inflammation and demyelination as well as axonal and neuronal degeneration. To date, effective therapies to reverse the disease are still lacking, so searching for biomarkers that could help distinguish the two mayor MS forms, relapsing-remitting (RRMS) and primary progressive (PPMS), is crucial. Increasing evidence indicates that dendritic cells (DCs) contribute to the pathogenesis of MS and might provide an avenue for therapeutic intervention. Therefore, in this study transcriptional profiling, in the basis of RNA-seq, of myeloid DCs (mDC) and plasmacytoid DCs (pDC) of 5 RRMS patients, 5 PPMS patients and 5 healthy controls was performed. Differentially Expressed Genes (DEG) analysis and Functional Enrichment Analysis demonstrated that there are many differences between the two multiple sclerosis forms in DCs. We were able to identify 20 genes that were differentially expressed between PPMS and RRMS patients in mDCs and > 100 in pDCs. Functional enrichment analysis also showed that the pathways identified as most significant were different in PPMS vs. RRMS between mDC and pDC.

RESUMEN

La esclerosis múltiple (EM) es una enfermedad autoinmune del sistema nervioso central (SNC) caracterizada por inflamación y desmielinización, así como por degeneración axonal y neuronal. Hasta la fecha, todavía faltan terapias efectivas para revertir la enfermedad, por lo que es crucial buscar biomarcadores que puedan ayudar a distinguir las dos formas principales de EM, remitente-recurrente (EMRR) y progresiva primaria (EMPP). La creciente evidencia indica que las células dendríticas (CD) contribuyen a la patogénesis de la EM y podrían proporcionar una vía para la intervención terapéutica. Por lo tanto, en este estudio se realizó el perfil transcripcional, en base a RNA-seq, de CD mieloides (mCD) y CD plasmocitoides (pCD) de 5 pacientes con EMRR, 5 pacientes con EMPP y 5 controles sanos. Los análisis de expresión genética diferencial y el análisis de enriquecimiento funcional demostraron que existen muchas diferencias entre las dos formas de esclerosis múltiple en las CD. Pudimos identificar 20 genes que se expresaron diferencialmente entre pacientes con PPMS y RRMS en mCD y > 100 en pCD. El análisis de enriquecimiento funcional también mostró que las vías identificadas como más significativas eran diferentes en PPMS frente a RRMS entre mCD y pCD.

2. INTRODUCTION

Multiple sclerosis (MS) is an autoimmune and neuroinflammatory disease of the central nervous system (CNS) in which the immune system attacks the myelin sheath wrapped around the axon resulting in neuronal dysfunction (Mutukula *et al*., 2021). It affects approximately 2.5 million people worldwide (Thompson *et al*., 2018), with most frequently onset of disease diagnosed between 20 and 40 years old. To date, there is still no cure for this condition (Calahorra *et al*., 2022). Additionally, studies determine that MS is more frequent in women and in northern locations (Flórez-Grau *et al*., 2018). MS can affect any part of the CNS, and thus, its clinical manifestations are often diverse, with signs and symptoms that vary widely depending on the extent and location of the damaged areas (Calahorra *et al*., 2022). However based on the clinical data and the histopathological studies three main clinical subtypes of MS have been described: relapsing-remitting multiple sclerosis (RRMS), the most common form, affecting approximately 85% of patients, is defined by acute exacerbations or relapses followed by a remission or a period of clinical recovery, and then recurring bouts of relapse and remission; primary progressive multiple sclerosis (PPMS), where disease progression occurs without remission, patients show progressive decline in neurological function since the time of disease onset. In this case, usually patients have a higher age of disease onset; and secondary progressive multiple sclerosis (SPMS), which is characterized by gradual progression after an initial relapsing remitting course. 80% of patients with RRMS eventually progress into SPMS approximately 20 years after diagnosis (Gandhi *et al*., 2010; Dendrou & Friese, 2015; Klineova & Lublin, 2018; Lassmann, 2019).

Although the exact causes of the disease and the mechanisms underlaying MS remain unknown, the infiltration of immune cells into de CNS in the presence of pre-existing genetic and environmental factors, such as vitamin D deficiency, ultraviolet B light (UVB) exposure, Epstein–Barr virus (EBV) infection, obesity and smoking could lead to increase disease susceptibility (Dobson & Giovannoni, 2019). Diverse studies have demonstrated that neuroinflammation in MS is associated with infiltration and accumulation of immune cells targeting myelin in the CNS. Although, generally both adaptive and innate immune cells are present in MS lesions, until recently MS research was mainly focused in the adaptive arm of the immune system (Nuyts *et al*., 2013). In fact, MS is considered to be predominantly a T-cell disease in which T cells are assisted by professional antigen-presenting cells, dendritic cells (DCs) (Xie *et al*., 2015). Immune dysregulation appears to originate with DCs which seem to have an activated phenotype in individuals with MS (Grigoriadis & Pesch, 2015). DCs provide an

important link between the innate and the adaptive immune system (Thewissen *et al*., 2014). These cells process antigens and present antigen peptide fragments on MHC (major histocompatibility complex) molecules to naïve T cells (Comabella *et al*., 2010). By secreting a number of cytokines, DCs play an important role in polarizing T cell responses and regulating the balance between immunity and tolerance (Cools *et al*., 2011). In the absence of inflammation, dendritic cells can induce tolerance by presenting autoantigens and environmental antigens to naive T cells. Mechanisms that confer T cell tolerance are diverse and include T cell deletion as well as the generation of T regulatory (Treg) cells. On infection or other causes of dendritic cell maturation, these cells enhance their antigen processing and presenting capacities and upregulate their production of cytokines and co-stimulatory molecules. Mature dendritic cells can induce naive T cells (Comabella *et al*., 2010). In MS, upon pathological activation of DCs in the periphery, activated T cells secrete proinflammatory cytokines facilitating their entry through the endothelial blood-brain barrier (BBB). Once in the CNS, these T cells are reactivated upon encounter of resident APCs, including DCs, presenting myelin derived epitopes. Subsequently, these T cells will secrete proinflammatory cytokines allowing recruitment of other inflammatory cells. This inflammatory cascade will lead to demyelination of axons, thereby causing the sensory and motor symptoms of MS (Nuyts *et al*., 2013).

Dendritic cells are a heterogenic population of leukocytes that originate from hematopoietic stem cells. They belong to the group of mononuclear phagocytes, consisting of macrophages, monocytes and dendritic cells (Balan *et al*., 2019). DCs are ubiquitous in the body, found in blood, tissues and lymphoid organs. In humans, there are two major subsets of DCs: myeloid or conventional DCs (mDCs or cDCs) and plasmacytoid DCs (pDCs). Myeloid dendritic cells consist of two subsets generally classified as conventional DC1 (cDC1) and conventional DC2 (cDC2). cDC1 is a subset with high expression of $CD141^+$ which are present at approximately one tenth the frequency of cDC2. They can also be identified by unique expression of C type lectin receptor 9A (CLEC9A) (Collin & Bigley, 2017). Moreover, cDC1 have a unique potential to induce cellular immunity against intracellular pathogens and malignant cells due to the processing and cross-presentation of exogenous antigens on MHC class I molecules to activate $CD8^+$ T cells and Th1 (T helper) cells (Fucikova *et al*., 2019). Unlike cDC1, cDC2 are the major population of myeloid DCs and are generally known as $BDCA1^+$ DCs or $CD1c^+$ DCs (Balan *et al*., 2019). They are known to be potent inducer of $CD4^+$ T cells response (Fucikova *et al*., 2019). pDCs are characterized by their unique ability to produce extremely high amounts of type I interferon (IFN) upon recognition of foreign nucleic acids (Balan *et al*., 2019). They express Toll

like receptor 7 and 9 (TLR7 and TLR9) as well as CD123, BDCA2(CD303), and BDCA4 (CD304), which can be used as markers to isolate them (Xie *et al*., 2015).

There is increasing evidence for a central role of DCs in MS. Several studies have demonstrated that there is abundant presence of both mDCs and pDCs in the inflamed CNS lesions and cerebrospinal fluid (CSF) of patients with MS (Nuyts *et al*., 2013). Both mDCs and pDCs accumulate in the leptomeninges and white matter lesions of MS patients. Individuals with MS have increased number of pDCs in CSF compared to healthy controls. The frequency of mDCs in CSF is dependent on disease duration. Highest frequencies of mDCs are found in patients with early MS, but then decrease over time (Serafini *et al*., 2006). Not only DC frequency, but also DC phenotype varies with the heterogenous clinical course of MS. Circulating mDCs of patients with RRMS display more pronounced expression of costimulatory markers, such as CD40 and CD80, which indicates a more proinflammatory phenotype compared to healthy controls. CD40 and CD80 are two costimulatory molecules implicated in the induction of immunity mediated by Th1 cells, the increased expression of these costimulatory markers may lead to higher production of proinflammatory interleukin (IL)-12, IL-18 and tumor necrosis factor (TNF)-α (Karni *et al*., 2006). In contrast, mDCs of patients with PPMS have a more immature phenotype compared with healthy controls, as indicated by reduced expression of the costimulatory molecules CD80 and CD86. Data also indicates that the production of proinflammatory cytokines such as IL-12, TNF-α and IL-23 is upregulated in both RRMS and SPMS patients. In fact, *in vitro* data, using monocyte derived DCs (MoDCs), confirms that cells from patients with MS secrete higher levels of proinflammatory cytokines IL-6, TNF-α and IL-23, than the MoDCs taken from healthy individuals (Huang *et al*., 2001). In contrast to mDCs, the phenotype of circulating pDCs of MS patients is more comparable with that of healthy controls (Serafini *et al*., 2006). Conflicting data has been presented with regard to the expression of costimulatory markers. Stasiolek *et al*., (2006) demonstrated that pDCs show a maturational defect and an altered immunoregulatory function in MS patients which might cause these cells to be less efficient in mounting an immune response. In individuals with MS, pDCs failed to efficiently express CD40, a molecule of crucial relevance for DC-T cell interactions. This study also described a reduced expression of CD86 and CD137 ligand on pDCs in RRMS patients compared with healthy controls (Stasiolek *et al*., 2006), while other studies indicate no differences (Lande *et al*., 2008). At the same time, cytokines produced by pDCs such as type I INF, IL-6, TNF-α seem to have been implicated in MS pathogenesis. Type I INF promotes Th1 polarization and IFN-γ production; IL-6 promotes myelin antigen-specific Th17 responses in encephalomyelitis (EAE) (animal model that resembles MS);

and TNF-α directly induces oligodendrocyte apoptosis and mediates human neuronal injury after activation with TLR9 agonists (Glehn *et al*., 2012).

In summary, peripherally derived dendritic cells that infiltrate the CNS seem to be crucial for the disease development. Moreover, evidence is emerging that overproduction of particular cytokines by DC subtypes drives autoimmune CNS inflammation. In contrast, some dendritic cells located in lymphoid organs have the capacity to confer antigen-specific tolerance to T cells and prevent the development of MS (Flórez-Grau *et al*., 2018). Since the role of dendritic cells is regulating the balance between immunity and tolerance, immunotherapies that target these cells by either inhibiting their immunogenic potential or enhancing their tolerogenic functions could provide benefits to patients with MS (Comabella *et al*., 2010). In fact, the therapeutic efficacies of diverse MS treatments are thought to be associated with modulation of the immunologic functions of DCs. Currently, there are treatment options for MS that can affect DC function and phenotype, but there is still no DC-based drug for treating MS. However, developing therapies that target DC, specially tolerogenic DCs, is an area of active investigation in MS (Xie *et al*., 2015). It is also important to underline that almost all of the drugs developed to treat MS are for patients diagnosed with RRMS. Patients with PPMS are considered to be less responsible to immunomodulatory therapies and are usually excluded from trials aimed at demonstrating drug efficacy. Subsequently they are then excluded from using the new therapies in PPMS patients (Gandhi *et al*., 2010).

As explained above, evidence is available that pathogenic mechanisms are different between the major forms of multiple sclerosis. From the study of these mechanisms, biomarkers that could be helpful in distinguishing between RRMS and PPMS may emerge (Lassmann, 2019). DCs also seem to be crucial for the development of this disease, both mDCs and pDCs appear to show different frequency, phenotype and expression in both MS forms (Nuyts *et al*., 2013). In fact, DCs have not yet been explored as a source of biomarkers for clinical course in MS. For this reason, biomarkers that can aid in the diagnosis, the differentiation of MS phenotypes, the monitoring of disease progression or in the monitoring of treatment response are needed (Iparraguirre *et al*., 2020). Although numerous advancements have been made in MS treatment, there is still no widely acceptable cure for MS. Understanding the precise molecular mechanism of MS is crucial to develop effective therapies. Whole genome transcriptome studies offer an opportunity to discover genes altered by MS or that may underlie the disease (Almsned *et al*. 2021).

For this reason, the aim of this study is to perform whole genome transcriptional profiling, in the basis of RNA sequencing (RNA-seq), of the two main categories of blood circulating dendritic cells, mDCs and pDCs, purified from peripheral blood mononuclear cells (PBMCs) of PPMS, RRMS patients and healthy controls (HC). This research may facilitate the discovery of biomarkers in DC that distinguish PPMS and RRMS, which have not been explored yet. The study might also ease the understanding of DC mechanisms in PPMS and RRMS and may uncover novel therapeutic targets for treating PPMS.

3. MATERIALS AND METHODS

3.1. Sample collection

Peripheral blood form PPMS and RRMS patients and healthy donors which had signed the informed consent was collected. All patients' samples were collected within the first five years of disease onset and patients had not started treatment yet. A total of 17 biological samples were collected for this study. 10 were from MS patients, which were collected from 2 different cohorts: Hospital Universitario de Cruces (HUC), Barakaldo and Hospital Universitario de Galdakao (HUG), Galdakao. 5 samples belonged to primary progressive MS (PPMS) patients and 5 to relapsing-remitting MS (RRMS) patients. 7 healthy donor samples were provided by the Biobanco Vasco. 5 samples were prepared for RNA-seq and 2 were used for quality control analyses. PPMS patients were 3 males and 2 females with a mean age of 51.8 (± 10.92) and RRMS patients were 2 males and 3 females with a mean age of 33 (± 6.24). The mean age of the healthy controls, which were all females, was 35.2 (± 9.95).

3.2. Isolation of myeloid dendritic cells and plasmacytoid dendritic cells

Myeloid DCs (mDCs) and plasmacytoid DCs (pDCs) were isolated from 17 samples. Four 10 ml EDTA tubes of peripheral blood were collected from each MS patient. Peripheral mononuclear cells (PBMCs) were isolated from approximately 40 ml of blood by Ficoll®-Plaque density gradient using 50ml SepMate™ tubes (STEMCELL Technologies, Ref. 85450). For that, total blood amount was measured, divided in 3 equal tubes and diluted in the same volume of PBS (Phosphate-buffered saline). Then, the diluted blood was pipetted down the side of a 50ml SepMate tube filled with 15ml of Ficoll®-Plaque and centrifugated at room temperature (RT) at 1200 x g for 10 minutes with the brakes on. During centrifugation differential migration results in the formation of layers containing different cell types. The bottom layer contains erythrocytes, the top layer plasma, and PBMCs and platelets are found in the interface between

plasma and the Ficoll®-Plaque. Plasma with PBMCs was quickly poured off into a new tube and 2 wash steps were performed in order to remove plasma and platelets. Then, PBMC concentration was determined with Trypan Blue. Before DC isolation $CD14^+$ monocytes were separated from PBMCs using CD14 Human MicroBeads (Miltenyi Biotec, Ref. 130-050-20). For that, first, PBMCs were centrifugated at 300 x g for 10 min at RT, then the supernatant was removed and the pellet was resuspended in 80µl of buffer (PBS pH 7.2, BSA 0.5%, EDTA 2mM) and 20µl CD14 MicroBeads per 10^7 total cells. The mixture was then incubated in the refrigerator for 15 min. After that, cells were washed by adding 6ml off buffer, centrifuged at 300 x g 10 min and resuspended in 500µl of buffer. A MS column (Miltenyi Biotec, Ref. 130-042-201) was placed in the magnetic field of a suitable MACS separator and the cell suspension was added into de column. Then 3 washing steps (3x500µl buffer) were performed. $CD14^+$ cells are positively selected and mDCs and pDCs are in the negative fraction that passes through the column. The negative fraction (2ml) was then divided into two equal parts and mDCs were isolated with EasySep™ Human Myeloid DC Enrichment Kit (STEMCELL Technologies, Ref. 19061) and pDCs with EasySep™ Human Plasmacytoid DC Enrichment Kit (STEMCELL Technologies, Ref. 19062) following "the Big Easy" magnetic protocol. In both cases DCs are negatively selected. The isolated pDCs and mDCs were stored in Qiagen RNA extraction kit's lysis buffer (QIAGEN, Ref. 74034) at -80°C.

3.3. RNA extraction and quantification

RNA was extracted from 16 samples of both mDC and pDC cells using the RNeasy Plus Micro Kit (QIAGEN, Ref. 74034) which is designed to purify small amounts of total RNA. RNA was extracted following the manufactures instructions and treated to eliminate genomic DNA (gDNA). Total RNA quality was assessed and its concentration was measured using the Agilent RNA 6000 Pico Kit (Agilent Technologies, Ref. 5067-1513) by the Agilent Technologies 2100 Bioanalyzer (Agilent Technologies). Electropherogram features for a successful sample run will be 1 marker peak and 2 ribosomal peaks: one for 18S and the other for 28S.

3.4. Quality controls of pDCs and mDCs isolation: flow cytometry and droplet digital PCR

To verify the purity of the isolated subpopulation, cells were analyzed by flow cytometry (MASCQuant® flow cytometer, Miltenyi Biotech) using CDc1-APC and DC141-VioBrightFITC antibodies for mDCs and C123-PE and DC303-APC antibodies for pDC. CD14-VioBlue antibody was used as a control for $CD14^+$ monocytes and CD19-PE for B cells. For the assessment of the purity, mDCs and pDCs from a healthy donor were extracted and kept in buffer (PBS pH 7.2,

2%FBS and 1Mm EDTA). Each DC population was divided into 5 tubes, since antibodies were analyzed separately. Then cells were centrifuged at 300 x g for 10 minutes, supernatant was removed and resuspended in 98µl of buffer. Then 2µl of required antibody was added. The solution was incubated at 4ºC for 10 minutes in the dark and then washed by adding 1ml of buffer, centrifuged at 300 x g for 10 min and finally resuspended in 200µl of buffer.

Droplet Digital PCR (ddPCR) was also performed in order to assess the quality of the isolated mDCs and pDCs form a healthy donor using the QX200™ Droplet Digital PCR System (Bio-Rad). First, RNA was extracted from both DC populations, the positive fraction generated in the extraction of the DCs (QC- mDC and QC- pDC, used as a negative control) and positively selected $CD14^+$ monocytes from PBMCs. Then, a RT-PCR was performed using the High-Capacity cDNA Reverse Transcription Kit in order to obtain the complementary DNA (cDNA) of the analyzed samples. For de ddPCR 25µl reaction mixes were prepared which consisted on 2x ddPCR SuperMix for Probes (No dUTP) (BioRad), 20x target primers/probe (FAM- or HEX/VIC-labeled) and cDNA (350pg). The probes against the genes of interest were FAM-labeled and the probe against the housekeeping gene was HEX-labeled (*Table 1*) (Bio-Rad). Each ddPCR assay mixture (20µL) was loaded into a disposable droplet generator cartridge (Bio-Rad). Then, 70µL of Droplet Generation Oil for probes (Bio-Rad) were loaded into each of the eight oil wells. The cartridge was then placed inside the QX200™ droplet generator (Bio-Rad). When droplet generation was completed (12,000 to 20,000 droplets), the droplets were transferred to a 96-well PCR plate using a Rainin multichannel pipet. The plate was heat-sealed with foil with the PX1™ PCR plate sealer (Bio-Rad) and then a PCR amplification was performed. In this case, the C1000 Touch™ Thermal Cycler (Bio-Rad) was used with the following thermal cycling conditions: 10 minutes at 95°C, 40 cycles of 30 seconds at 94°C and 60 seconds at 60°C and 1 cycle of 10 min at 98°C with a 2°C/s ramp rate. The droplets were read individually with the QX200™ Droplet Reader (Bio-Rad) and quantified with QuantaSoft droplet reader software (Bio-Rad). Positive droplet populations were separated from negative droplets and quantified as copies/µl (c/µl).

Table 1. FAM- and HEX- labeled probes used in the ddPCR

FAM-labeled probes	HEX-labeled probes
CD303 (pDC)	GAPDH (housekeeping)
CD123(pDC)	
CD1c (cDC2)	
CLEC9A (cDC1)	
CD14 ($CD14^+$ monocytes)	
CD19 (B cells)	

3.5. Preparation of cDNA libraries for RNA sequencing

The RNA library construction consisted of only high-quality RNA samples with RNA integrity number (RIN) over 8 and a concentration range between 2pg and 200ng. 30 libraries (15mDC, 15pDC) were generated by the NEBNext Single Cell/Low Input RNA Library Prep Kit for Illumina® (New England BioLabs, Ref. E6420S/L) following the Low Input RNA protocol. For the preparation of the libraries all RNA samples were normalized to 750pg/µl. Reverse Transcription and cDNA amplification were performed using the C1000 Touch™ Thermal Cycler (Bio-Rad). NucleoMag® NGD Clean-up and Size Select (Macherey-Nagel, Ref. 744970.50) magnetic beads were used for cleaning up the amplified DNA. Then, the amplified cDNA quality and quantity was assessed by the Agilent Technologies 2100 Bioanalyzer using the DNA High Sensitivity Kit (Ref. 5067-4626). cDNA fragmentation and adaptor-ligation were also performed with the C1000 Touch™ Thermal Cycler (Bio-Rad) and NucleoMag® beads were used for the cleaning up of the adaptor-ligated DNA. Finally, a PCR enrichment was performed using NEBNext® Multiplex Oligos for Illumina® (Dual Index Primers Set 1) (New England BioLabs, Ref. E7600S), which was followed by the last clean up with the NucleoMag® beads. The quality and quantity of the generated libraries was assessed by the Agilent Technologies 2100 Bioanalyzer using the DNA High Sensitivity Chip. Good quality libraries were considered those which the electropherogram showed a narrow distribution with a peak size of 300-350bp. Full transcriptomic sequencing of the libraries was done with the Illumina platform NovaSeq 6000 S4 (2X150) at CCGA Kiel Center in Germany. The libraries were sequenced in 1 lane of the NovaSeq 6000 S4, which can generate 2 billion of reads per lane.

3.6. Transcriptomic analysis of the sequenced libraries

Sequenced data was informatically analyzed at different levels in collaboration with Sistemas Genómicos. A quality control of the raw data was performed using the FastQC tool, which reports the quality profile of the sequenced reads (http://www.bioinformatics.babraham.ac.uk/projects/fastqc). Then reads were mapped against the latest version of *Homo sapiens* (GRCh38) genome, provided by NCBI database using Tophat 2.1.0. In whole transcriptome sequencing process, the number of mapped reads should be between 60-80% of total sequenced reads. Subsequently low-quality mapped reads were removed using Samtools 1.2 and Picard Tools 2.9.0. After selecting the reads with the highest mapping quality values, assembly and gene identification was performed using Bayesian inference methods with Cufflinks v2.2.1. In this step, the GC distribution, the proportion of guanine and cytosine bp along the reads, was also assessed, which should be centered between

40-60%. Finally, differential expression and functional studies between samples were performed to study the concordance between samples. These studies give us an idea of global transcriptomic correlation between samples. For this, a Pearson correlation study between samples for each condition was performed considering all the normalized transcriptome by library size and gene length. This process was realized using statistic programming language R [http://www.r-project.org/]. This type of analysis allows identifying abnormal biological replicates for each condition. To achieve the differential expression study between groups of samples (PPMS vs RRMS, MS vs HC), different Python and R statistic packages were used. Genes that are differentially expressed between conditions will be identified using the DESeq2 method. DESeq2 uses a negative binomial distribution as a dispersion model for the statistical significance (Love *et al*., 2014). A gene was considered differentially expressed if it had a FoldChange value lower than -1.5 or superior to 1.5 with an FDR adjusted *p*-value (p_adj-value) of 0.05 or smaller. Functional enrichment of differentially expressed genes for each condition was performed by over-representation test using R scripts using clusterProfiler, AnnotationHub, DOSE, pathview and rtracklayer.

4. RESULTS

4.1. Quality controls of the isolated myeloid and plasmacytoid dendritic cells.

Flow cytometry was used in order to assess the purity of the isolated fractions. In the case of plasmacytoid DCs a purity of approximately 90% was obtained and in the case of myeloid DCs 86%. 78.07% of the mDCs were positive for CD1c antibody, a marker for cDC2 subset, and 8.51% were positive for CD141, a marker for the cDC1 subset. Both $CD1c^+$ and $CD141^+$ together constitute the mDC population. In this population $CD14^+$ cells accounted for only 6% of the isolated fraction and $CD19^+$ cells (mainly B cells) were practically undetectable *(Figure 1*). In the case of pDCs, 90.82% of cells were positive for CD123 marker and 92.19% were $CD303^+$. In this population $CD14^+$ monocytes were practically undetectable and B cells ($CD19^+$) were only 6% (*Figure 2*).

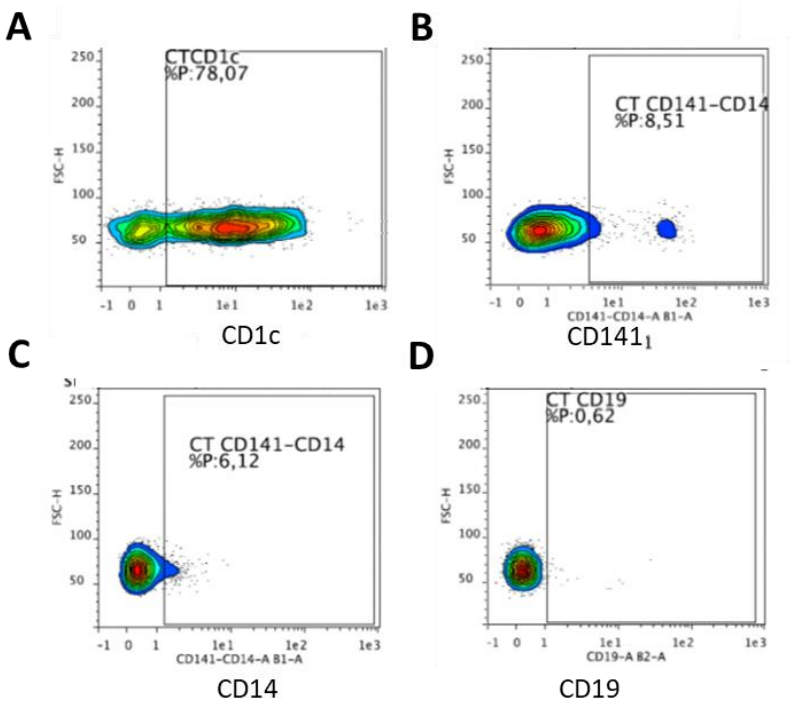

Figure 1. Graph of flow cytometry of the isolated mDCs from a healthy donor. (A) and (B) show $CD1c^+$ and $CD141^+$ staining in mDC isolated fraction. (C) and (D) represent the % of $CD14^+$ and $CD19^+$ cells, respectively.

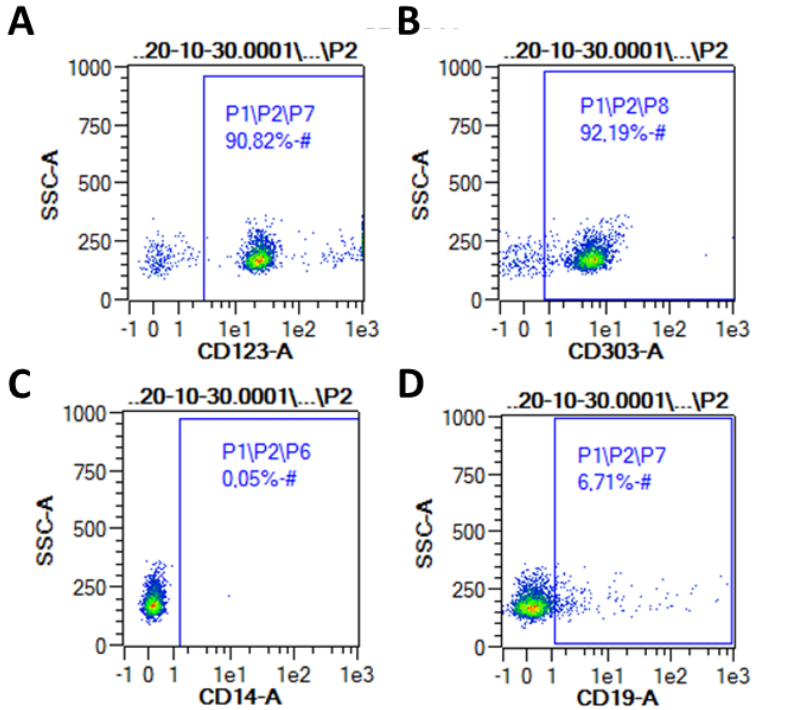

Figure 2. Graph of flow cytometry of the isolated pDCs from a healthy donor. (A) and (B) show $CD123^+$ and $CD303^+$ staining in pDC isolated fraction. (C) represents the % of $CD14^+$ cells and (D) exhibits the % of B-cells.

In addition to cytometry quality control, gene expression pattern of known markers in the isolated pDC and mDC fractions was tested to validate their purity using droplet digital PCR (ddPCR). Plasmacytoid DCs fraction only showed expression for the subset specific markers: 138.5c/µl of CD303 and 39.7c/µl of CD123. Myeloid DCs fraction showed a high expression of cDC2 subpopulation's specific marker CD1c (51c/µl). CLEC9A, a specific marker for the cDC1, was not expressed in any of the analyzed fractions. CD303 and CD123 were also expressed in the mDC fraction, but in low levels, 15.55c/µl and 5.35c/µl, respectively. Positively selected $CD14^+$ cells from PBMCs showed a high expression of the subset specific marker CD14 (544c/µl), but in this fraction mDC specific marker CD1c was also expressed at low levels (5.4c/µl). The other analyzed fractions did not express CD14 marker, except mDCs that showed a very low expression of CD14 marker (1.8c/µl). B cells specific marker CD19 was not expressed in any of the analyzed fractions.

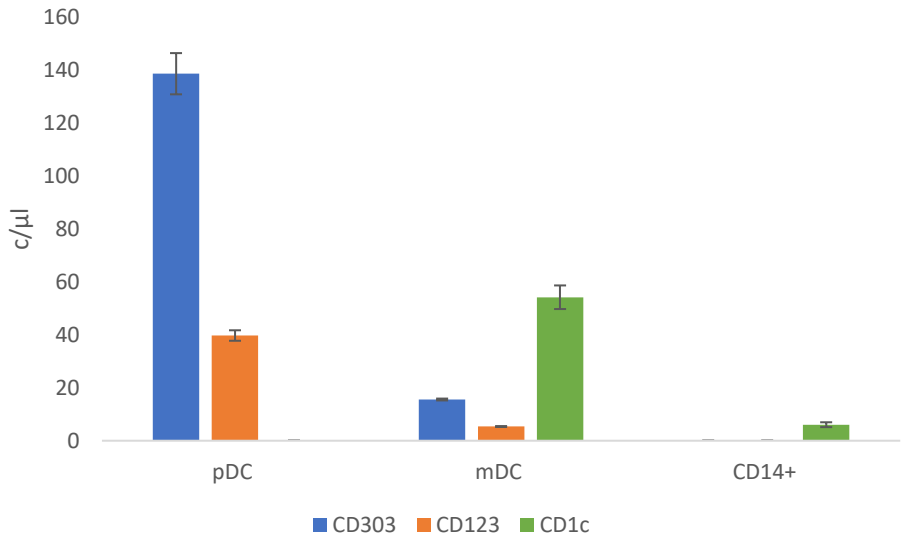

Figure 3. Gene expression quantification by droplet digital PCR of a healthy donor's sample. Bar graph shows mean values of 2 replicates of mDC, pDC and $CD14^+$ monocytes mRNA transcript counts of CD303, CD123 and CD1c in c/µl. Standard deviation is also presented.

4.2. Library construction data

Global yield of RNA obtained from the isolated pDCS and mDCS was low (*Table 1*), but the RNA extracted from the isolated mDCs and pDCs met the high-quality requirements for library construction (*Figure 4A*). All the samples used for this study had a RIN ≥ 8. Libraries generated with NEBNext Single Cell/Low Input RNA Library Prep Kit for Illumina® met the manufacturers' quality requirements (*Figure 4B*) and in all cases the obtained cDNA concentration was enough to sequence the libraries (*Table 2*).

Table 2. RNA and library cDNA quantification. Averages of RNA concentration and of library concentration from 5 samples of each group

Sample Name	Average RNA concentration (pg/µl)	Average library concentration (ng/µl)
mDC-PPMS	1244.4	15.54
pDC-PPMS	1025.2	9.94
mDC-RRMS	1352	50.74
pDC-RRMS	430.4	23.22
mDC-HC	1505.2	14.26
pDC-HC	2482.5	10.2

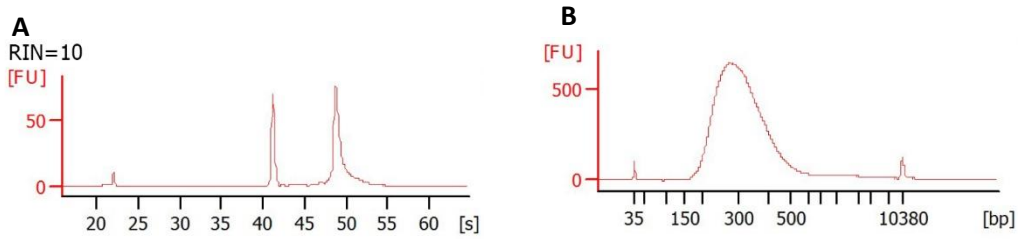

Figure 4. RNA and library cDNA electropherograms of mDC-RRMS_3 sample. (A) shows RNA electropherogram with two peaks for 18S and 28S and a RIN value of 10 and (B) shows library cDNA electropherogram with a narrow distribution and a peak size of approximately 350bp.

4.3. Quality of the analyzed data

FastQC tool evaluates the quality of the raw data to ensure there are no biases that may affect how the data can be usefully used. It aims to provide a quality control report which can spot problems which originate either in the sequencer or in the starting library material. For each sequenced library 2 FastQC reports were obtained, one corresponding to the forward read and other to the reverse, so in total 60 FastQC reports were obtained. For this reason, all figures presented in the library quality resultS are considered representative figures. One of the most important estimator analyses of the FastQC tool is the Per Base Sequence Quality Analysis which shows and overview of the quality values across all bases of the data. High quality libraries are considered those whose quality values (Phred values) are higher than 20. All the libraries constructed with the Low Input RNA Library Kit were considered high quality libraries since all the calls had quality values higher than 20. As we can see in *Figure 5*, quality values stay in the green area but as the read gets longer base calls fall into the orange area. It is common to see

base calls falling to this area towards the end of a read since the quality of calls will degrade as the run progresses.

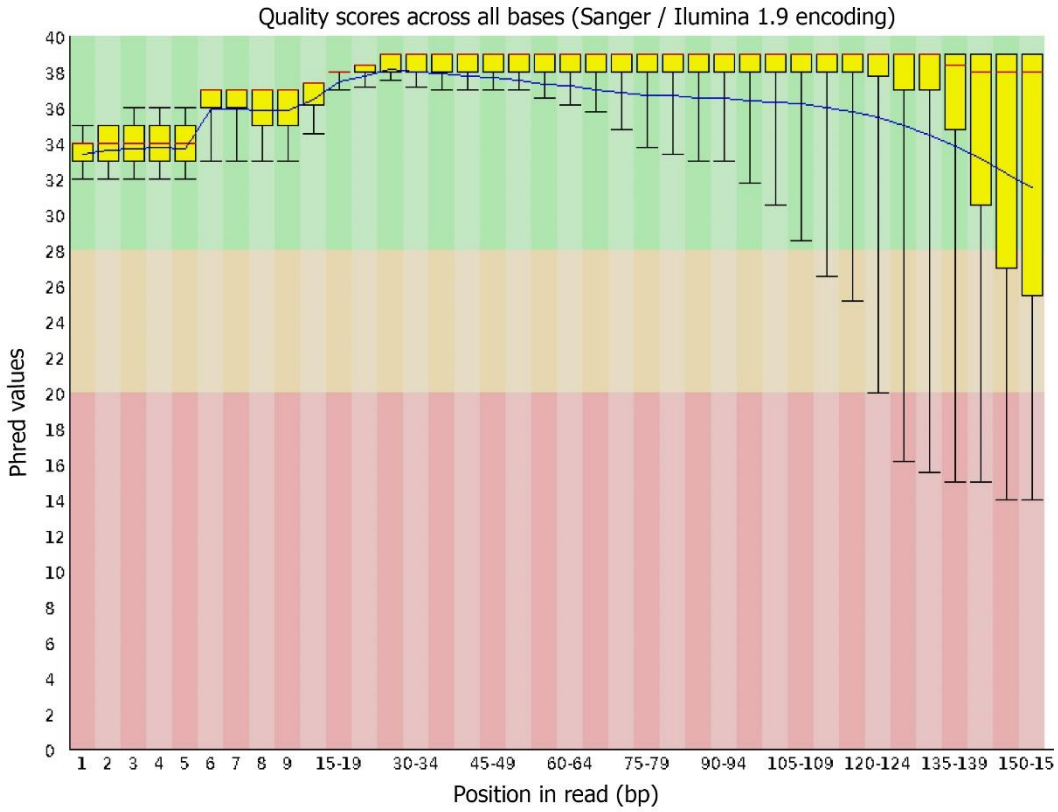

Figure 5. Representative boxwhisker type plot of per base sequence quality of the constructed libraries with the Low Input RNA library Kit. The y-axis on the graph shows the Phred values (quality scores) of the base calls and the x-axis the position in the read (bp). Yellow boxes represent the interquartile range (25-75%) and the upper and lower whiskers represent the 10% and 90% points. The central red line is the median quality value and the blue line represents the mean quality. The background of the graph divides the y axis into very good quality calls (green), calls of reasonable quality (orange), and calls of poor quality (red).

As mentioned before, as a rule in whole transcriptomic sequencing, the number of mapped reads should oscillate between 60-80% of total sequences reads. In this case, the 30 mapped samples showed normal-to-high values. In fact, same samples had a number of mapped reads which were above the 80% of total sequence reads (*Table 3*).

In addition, GC content distribution was calculated. Results show that the GC content of all sequenced libraries was between the desired distribution values, which implied that all samples presented a normal GC distribution value between 40-60%. FastQC tool calculates the GC distribution of the libraries across the whole length of each sequence and compares it to a

modelled normal distribution of GC content. In this case, as shown in *Figure 6*, our samples' GC content (red line) is shifted toward lower GC content compared to the theoretical distribution (blue line), but the central peak is still between the 40-60% range. The central peak of our samples' GC distribution is over the theoretical peak which might indicate contamination. However, in our case it is considered a specific contaminant as will be seen in further FastQC analysis, it is probably related to the index primers used in library construction.

Table 3. Mapped read statistics of the 30 libraries. Sample name, total number of mapped read and high-quality percentage (%HQ) of mapped reads are shown.

Sample	#Mapped Reads	%HQ mapped
mDC-PPMS_1	68456890	78%
mDC-PPMS_2	59345612	76%
mDC-PPMS_3	73987172	78%
mDC-PPMS_4	39012398	69%
mDC-PPMS_5	64017888	73%
pDC-PPMS_1	43987612	70%
pDC-PPMS_2	60470458	68%
pDC-PPMS_3	62090704	81%
pDC-PPMS_4	78570208	74%
pDC-PPMS_5	48190043	79%
mDC-RRMS_1	76950398	77%
mDC-RRMS_2	83429841	82%
mDC-RRMS_3	89369284	81%
mDC-RRMS_4	92498727	79%
mDC-RRMS_5	69399837	69%
pDC-RRMS_1	65819713	73%
pDC-RRMS_2	66669510	74%
pDC-RRMS_3	58654981	81%
pDC-RRMS_4	79604746	73%
pDC-RRMS_5	42121480	71%
mDC-HC_1	64766821	81%
mDC-HC_2	47349950	83%
mDC-HC_3	69931684	78%
mDC-HC_4	72513419	71%
mDC-HC_5	69095153	82%
pDC-HC_1	52323111	75%
pDC-HC_2	62998480	81%
pDC-HC_3	56157280	71%
pDC-HC_4	67723950	82%
pDC-HC_5	59974553	77%

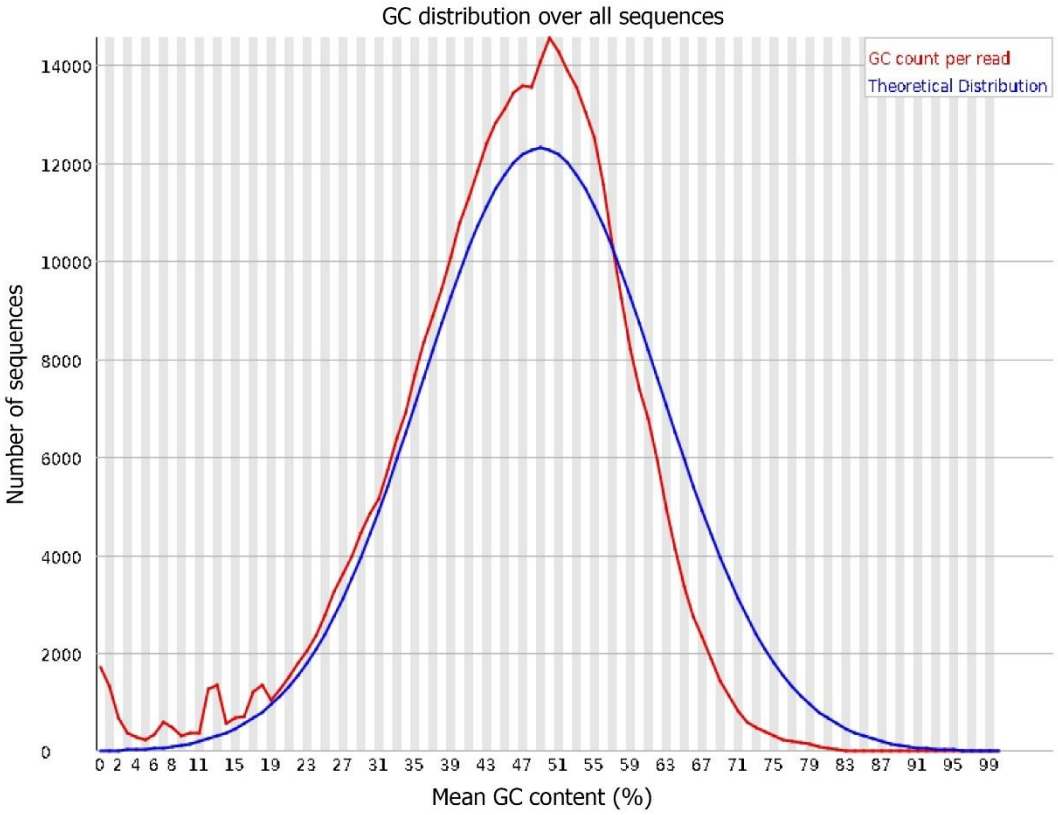

Figure 6. Representative GC distribution over all sequences. The y-axis represents the number of sequences and the x-axis the mean GC content. Red line indicates GC count per read of the analyzed samples and blue line indicates a theoretical distribution.

All samples also presented optimal values for duplication distribution. This parameter is an indicator of sequencing process quality. In fact, it could indicate degradation of source biological material, or may also indicate significant deviations in sequencing process. FastQC tool also analyzes the duplication level of the sequenced libraries. In this case, two duplicated spikes can be seen across the blue line one around 10 and other around 5.000 (*Figure 7*). The plot also gives an expected overall loss of sequence were the library to be deduplicated. The sequenced libraries will not pass the quality control if the overall level of loss is higher than 50%. FastQC tool analyses the duplicated sequences that individually represent more than the 0.1% of the overall library and compare them to sequences of possible source of contamination. In this case, all the overrepresented sequences belong to the index primers used in library construction.

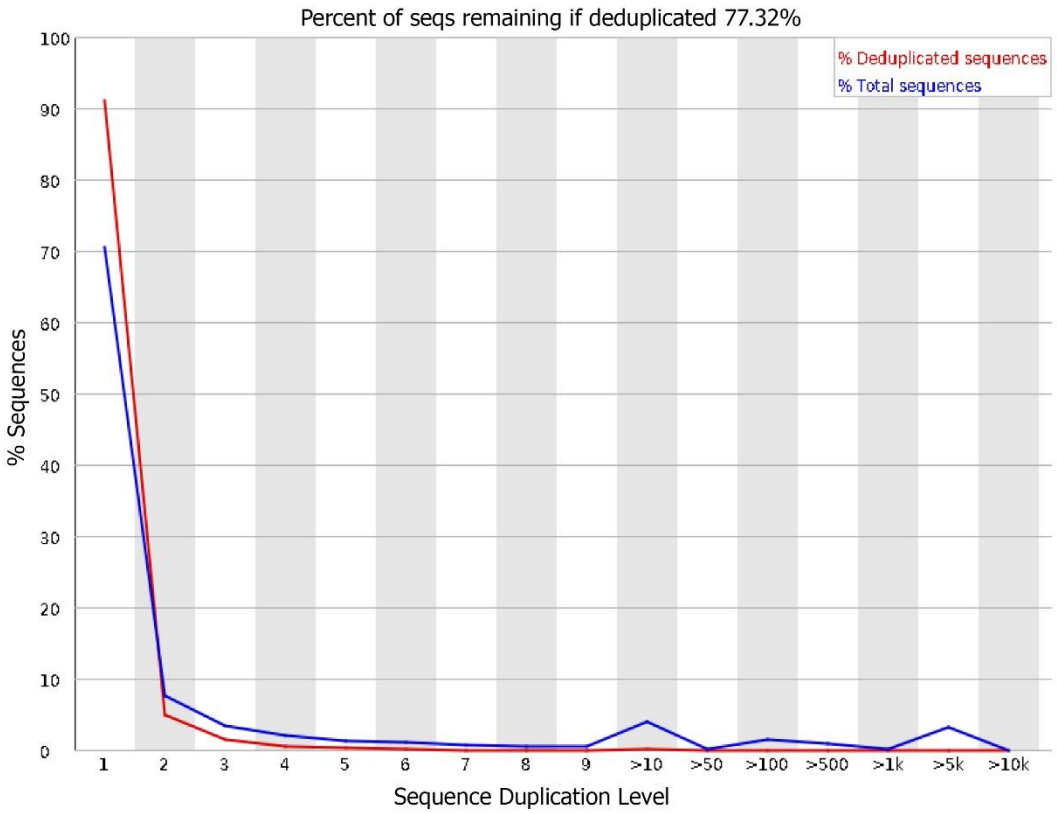

Figure 7. Representative duplication levels of the sequenced libraries. The y-axis shows the % of sequences and the x-axis the sequence duplication level. Blue line represents the percentage of duplication levels of the total analyzed libraries and red line indicates de percentage of deduplicated sequences. Plot also provides the percentage of remaining sequence if libraries were deduplicated.

Due to the nature of RNA-seq sequencing gene length and size of library by sample may influence the subsequent statistical analysis of the data. Elimination of different statistical deviations can be achieved by normalizing the quantification data. In our case, the normalization step improved considerably the homogeneity of the distributions in all conditions. In *Figure 8* the normalized distribution of gene expression in a selection of our libraries can be observed.

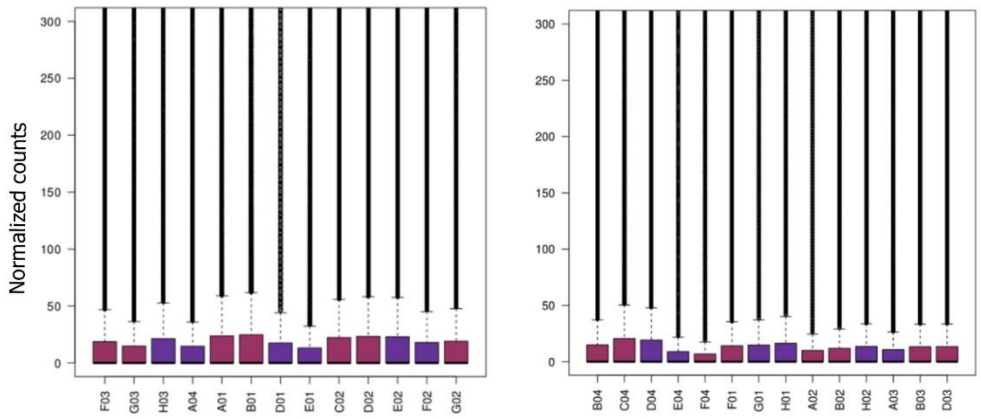

Figure 8. Normalized distribution of gene expression in a selection of constructed libraries, mDC (left) and pDC (right). y-axis shows normalized counts by library and gene size and in x-axis a selection of samples.

DEesq2 algorithm was chosen to identify the differentially expressed genes between condition. This algorithm is one of the most conservative methods used in RNA-seq. It uses a negative binomial distribution which is needed to confirm the corrected fitted of each differential expression with the theorical distribution. In our study, the theoretical model fitted the experimental distribution of gene dispersion in all cases.

4.4. Differentially Expressed Genes (DEG) and Functional Enrichment analysis.

Results revealed many differently regulated genes between the compared groups: PPMS vs RRMS and MS vs HC. We were able to identify 20 genes that are differentially expressed between PPMS and RRMS patients in mDCs and > 100 in pDC. Comparison between the two multiple sclerosis forms and healthy controls also showed DEG (*Table 4*).

Table 4. Statistics of the Differential Gene Expression analysis. Fold Change values, P adjusted values and the number of significant DEG are provided.

DC Type	Group 1	Group 2	Fold Change Min between Groups	Fold Change Max between Groups	*P_adj*-Value Lowest	*P_adj*-Value Highest	Number of Significant DEG
mDC	PPMS	RRMS	1.8	77	3.85E-08	0.044	20
pDC	PPMS	RRMS	1.8	85	7.37E-13	0.049	> 100
mDC	PPMS	HC	1.5	30	1.98E-10	0.048	26
pDC	PPMS	HC	4.5	36	1.06E-08	0.048	15
mDC	RRMS	HC	1.8	13	4.17E-13	0.049	> 100
pDC	RRMS	HC	1.6	99	1.17E-10	0.048	> 100

Functional enrichment analysis in PPMS vs RRMS group comparison showed different results between mDCs and pDCs. In mDCs based on "GO: Cellular Component" membrane-related processes, such as plasma membrane, transmembrane transporter, membrane rafts, membrane microdomain, etc were identified as the most significant components in this group comparison. Functional enrichment analysis based on "GO: Biological Process" identified MyD88-independent TLR signaling pathway as most significant category. In pDCs, significant "GO: Cellular Component" categories are ribosomal subunit and mitochondrial protein-containing complex, and significant "GO: Biological Process" categories include ATP-synthesis-coupled proton transport.

5. DISCUSSION

Multiple sclerosis is a complex disease, whose physiopathology is still not completely understood. Nevertheless, growing evidence supports a dysregulation of the immune system (Grigoriadis & Pesch, 2015). Evidence shows that dendritic cells play an important role in the pathogenesis of the disease (Collin & Bigley, 2017). Furthermore, the existing therapeutic available options for treating this disease are still limited (Stephen *et al*., 2020). For those reasons, it would be especially useful to identify biological markers that could facilitate the understanding of disease mechanisms or that might uncover novel therapeutic targets.

RNA sequencing is a powerful new method for mapping and quantifying transcriptomes developed to analyze global gene expression. This technique provides insights at multiple levels into the transcription of the genome, as it yields information about the sequence and expression-levels. It provides a far more precise measurement of levels of transcripts than other methods (Wang *et al*., 2009). In fact, RNA-seq technologies have been used as promising means for biomarker identification in MS. Studies in several immune cells have been performed, such as, in B cells, monocytes, T cells and leukocytes, but all of them have focused on comparing RRMS and HC (Ramesh *et al*., 2020; Almsned *et al*., 2021; Fernandes *et al*., 2019; Iparraguirre *et al*., 2020). However, a systematic whole-genome transcriptomic profiling of blood DCs has not been performed in MS, and DC transcriptional studies involved in PPMS versus RRMS are undocumented. This is why, the main objective of this study was to perform whole-genome gene expression profiling by means of RNA-seq in the two major blood DC subsets; pDCs and mDCs, purified from PBMC of PPMS and RRMS patients, and healthy controls.

Obtaining a good purification of DCs was very important step in this study, so we checked if our purified fractions contained no or minimal amounts of B cells and $CD14^+$ monocytes, the most likely contaminants in this purification procedure. Quality control performed by flow cytometry showed that the mDC and pDC fractions isolated with the EasySep™ Human myeloid/plasmacytoid DC enrichment Kits exhibited high purity values. In the case of mDC we obtained a purity of 86% and in pDCs approximately of 90%. In the mDC fraction 6% of cells were stained with CD14 antibody, but in pDCs $CD14^+$ population was practically undetectable (0.05%) (*Figure 1, Figure 2*). $CD14^+$ cells are positively selected when isolating cells from PBMCs and should not be detected or in very low amounts in other fractions. Phenotyping studies and single-cell gene expression studies have recently identified a small percentage of the $CD1c^+$ cDC2 population that express CD14, which have been characterized as monocyte-like DC (Villani *et al*., 2017). Therefore, it could be possible that this $CD14^+$ cells belong to those mDCs that express CD14.

ddPCR quality control was performed in order to validate the purity of the isolated DCs by analyzing the gene expression pattern of known markers. pDCs only showed expression for the subset specific markers, CD303 and CD123. mDCs, expressed the specific marker of the cDC2 subpopulation, but not of the cDC1 (CLEC9A). It could have been expected since the latter is considered an unusual fraction (Balan *et al*., 2019), although, in flow cytometry was detected in a very low percentage. Furthermore, mDCs also expressed CD303 and CD123, markers that are considered pDC-specific, in line with protein atlas (https://www.proteinatlas.org/). However, several studies have identified $CD303^+$ and $CD123^+$ myeloid DCs. In fact, CD303 is a myeloid DC precursor component so it overlaps in expression with pDCs (Villani *et al*., 2017) and $CD123^+$ mDCs represent earlier-stage immature mDC subset (Shi *et al*., 2008), but in both cases the highest expressing cells will include pDCs (Collin & Bigley, 2017). Positively selected $CD14^+$ monocytes from PBMCs were also analyzed in the ddPCR, and apart of expressing CD14, they also manifested CD1c marker. Schroder *et al*., (2016) demonstrated that a small fraction of classical and intermediate human monocytes also express CD1c. When analyzing this gene in protein atlas, it is also expressed in monocytes but in much lower proportions than in myeloid dendritic cells (https://www.proteinatlas.org/). Moreover, some cDC2 also express CD14 (Villani *et al*., 2017) so we hypothesize that it could be possible that when separating $CD14^+$ monocytes, purification of $CD14^+$ cDC2 is also happening. Further testing should be performed to understand if those $CD14^+$ cells expressing cDC2-specific considered markers are mDCs or monocytes. Flow cytometry would be a really interesting tool for this purpose.

Once the purity of the mDCs and pDCs was assessed we continued with the construction of the cDNA libraries. Bioanalyzer results showed that the RNA extracted from all samples met the high-quality requirement for library construction, since all had a RIN ≥ 8, but the obtained concentration was really low. However, it was enough for library construction (*Figure 4A*). Sequenced libraries were informatically analyzed in different levels. The 60 FastQC reports showed that in general sequenced libraries were considered high quality. Per Base Sequence Quality Analysis by FastQC tool showed that libraries presented high quality values since all the calls had quality values higher than 20 and when reads got longer although quality values were lower, they were still above 20 Phred values (*Figure 5*). Base calls quality falling lower in the Phred values towards the end of a read is common since the quality of the calls will degrade as the run progresses (Babraham Bioinformatics). This could be improved after quality trimming the adapters (Pollier *et al*., 2013). Mapped reads values also were considered normal-to high since in all cases they oscillated between the 60-80% of total sequences and in some cases even were above the 80% range (*Table 3*).

Libraries in general showed a GC distribution shifted to lower GC content compared with the theorical distribution but in all cases the GC content was between the desired distribution values, between the 40-60% range (*Figure 6*). Duplication distribution values were also optimal in all samples, although some duplication spikes were detected along the reads (*Figure 7).* FastQC tool detects two potential contamination sources in a library sample, contamination arising from PCR artefacts or cross contamination with other biological samples (Babraham Bioinformatics). In our case, GC distribution peak being above the theorical peak and having some duplication peaks could mean possible contamination, but in this case detecting biological information from another source should be difficult since all samples belong to humans. However, to check that, FastQC tool analyses the sequences that individually represent more than 0,1% of the overall library and compare them to sequences of possible source of contamination. In this case, this analysis confirmed that the possible contamination in our libraries belonged to the index primers or adapters used in library construction. The detected adapter sequences do not influence the subsequent analysis of the data and they could be informatically eliminated if we desired to. In summary, all these quality analyses confirm that the libraries are of good quality.

Differentially Expressed Genes (DEG) and Functional Enrichment Analysis demonstrated that there are many differences between the two multiple sclerosis forms in DCs. We were able to identify 20 genes that were differentially expressed between PPMS and RRMS patients in

mDCs and > 100 in pDCs. Some of these DEG reached high levels of significance and showed high fold-change differences between PPMS and RRMS, which makes them good biomarker candidates. Comparing the MS forms with healthy controls also showed DEG in both mDCs and pDCs (*Table 4*). Functional enrichment analysis also showed that the identified as most significant pathways based on "GO: Cellular Component" and "GO: Biological Process" were different in PPMS vs RRMS between mDCs and pDCs.

In conclusion, transcriptome studies of mDCs and pDCs in PPMS and RRMS seem promising. In fact, some of the DEG that were identified are already known in MS pathology, though not specifically in relation to DC. Interestingly, many genes we identified have not been specifically reported in MS pathology. However, MS is a heterogenous disease affecting approximately 2.5 million people worldwide, so with the aim of finding biomarkers that facilitate a better understanding of dendritic cell effector mechanisms in PPMS versus RRMS, and that may uncover novel therapeutic targets for treatment of MS, but specially PPMS, a larger group of patients should be considered for a whole transcriptome study. Considering a higher number of participants could change the most significant DEG or enriched pathways, but, even so, it can be concluded that there are differences between the two main blood DC population in PPMS and RRMS.

6. REFERENCES

Almsned F., Lipsky R. H., Jafri M. S. (2021). Transcriptomic analysis of Multiple Sclerosis patient-derived monocytes by RNA-sequencing for candidate gene discovery. *Informatics in Medicine Unlocked,* 23: 100563. Doi: 0.1016/j.imu.2021.100563

Babraham Bioinformatics- FastQC a quality control tool for high throughput sequence data. http://www.bioinformatics.babraham.ac.uk/projects/fastqc/

Balan S., Saxena M., Bhardwaj N. (2019). Dendritic cell subsets and locations. *International Review of Cell and Molecular Biology*, 348: 1-68. Doi: 10.1016/bs.ircmb.2019.07.004.

Calahorra L., Camacho-Toledano C., Serrano-Regal M. P., Ortega M. C., Clemente D. (2022). Regulatory cells in multiple sclerosis: from blood to brain. *Biomedicines*, 10 (2): 335-361. Doi: 10.3390/biomedicines10020335

Collin M., Bigley V. (2017). Human dendritic cell subsets: an update. *Immunology*, 154: 3-20. Doi: 10.1111/imm.12888

Comabella M., Montalban X., Münz C., Lünemann J. D. (2010). Targeting dendritic cells to treat multiple sclerosis. *Nature Reviews Neurology*, 6: 499-507. Doi: 10.1038/nrneurol.2010.112

Cools N., Petrizzo A., Smits E., Buonaguro F. M., Tornesello M. L., Berneman Z., Buonaguro L. (2011). Dendritic cells in the pathogenesis and treatment of human diseases: a Janus Bifrons? *Immunotherapy*, 3 (10): 1203-1222. Doi: 10.2217/imt.11.110.

Dendrou C., Friese M. (2015). Immunopathology in multiple sclerosis. *Nature Reviews*, 15 (9): 545-558. Doi: 10.1038/nri3871

Dobson R., Giovannoni G. (2019). Multiple sclerosis- a review. *European Journal of Neurology*, 26: 27-40. Doi: 10.1111/ene.13819

Fernandes S. J., Morikawa H., Ewing E., Ruhrmann S., Joshi R. N., Lagani V., … Gomez-Cabrero D. (2019). Non-parametric combination analysis of multiple data types enables detection of novel regulatory mechanisms in T cells of multiple sclerosis patients. *Scientific Reports*, 9: 11996. Doi: 10.1038/s41598-019-48493-7

Flórez-Grau G., Zubizarreta I., Cabezón R., Villoslada P., Benitez-Ribas D. (2018). Tolerogenic dendritic cells as a promising antigen-specific therapy in the treatment of multiple sclerosis and neuromyelitis optica from preclinical to clinical trials. *Frontiers in Immunology*, 9: 1169. Doi: 10.3389/fimmu.2018.01169

Fucikova J., Paloba-Jelinkova L., Bartunkova J., Spisek R. (2019). Induction of tolerance and immunity by dendritic cells: mechanisms and clinical applications. *Frontiers in Immunology,* 10: 2393. Doi: 10.3389/fimmu.2019.02393

Gandhi K. S., McKay F. C., Cox M., Riveros C., Armstrong N., Heard R. N., … Booth D. R. (2010). The multiple sclerosis whole blood mRNA transcriptome and genetic associations indicate dysregulation of specific T cell pathways in pathogenesis. *Human Molecular Genetics*, 19 (11): 2134-2143. Doi: 10.1093/hmg/ddq090

Glehn F., Santos L. M., Balashov K. (2012). Plasmacytoid dendritic cells and immunotherapy in multiple sclerosis. *Immunotherapy*, 4 (10): 1053–1061. Doi: 10.2217/imt.12.117.

Grigoriadis N., Pesch V. (2015). A basic overview of multiple sclerosis immunopathology. *European Journal of Neurology*, 22 (2): 3-13. Doi: 10.1111/ene.12798

Huang Y. M., Stoyanova N., Jin Y. P., Teleshova N., Hussien Y., Xiao B. G., … Link H. (2001). Altered phenotype and function of blood dendritic cells in multiple sclerosis are modulated by IFN-β and IL-10. *Clinical and Experimental Immunology*, 124 (2): 306-314. Doi: 10.1046/j.1365-2249.2001.01504.x

Iparraguirre L., Alberro A., Sepúlveda L., Osorio-Querejeta I., Moles L., Castillo-Triviño T., … Otaegui D. (2020). RNA-seq profiling of leukocytes reveals a sex-dependent global

circular RNA upregulation in multiple sclerosis and 6 candidate biomarkers. *Human Molecular Genetic*s, 29 (20): 3361-3372. Doi: 10.1093/hmg/ddaa219

Karni A., Abraham M., Monsonego A., Cai G.,Freeman G. J., Hafler D., … Weiner H. L. (2006). Innate immunity in multiple sclerosis: myeloid dendritic cells in secondary progressive multiple sclerosis are activated and arive a proinflammatory immune response. *Journal of Immunology*, 177 (6): 4196-4202. Doi: 10.4049/jimmunol.177.6.4196.

Klineova S., Lublin F. D. (2018). Clinical course of multiple sclerosis. *Cold Spring Harbor Perspectives in Medicine*, 8 (9): a028928. Doi: 10.1101/cshperspect.a028928

Lande R., Gafa V., Serafini B., Giacomini E., Visconti A., Remoli M. E., … Coccia E. M. (2008). Plasmacytoid dendritic cells in multiple sclerosis: intracerebral recruitment and impaired maturation in response to interferon-beta. *Journal of Neuropathology and Experimental Neurology*, 67 (5): 388-401. Doi: 10.1097/NEN.0b013e31816fc975.

Lassmann H. (2019). Pathogenic mechanisms associated with different clinical courses of multiple sclerosis. *Frontiers in Immunology*, 9: 3116. Doi: 10.3389/fimmu.2018.03116.

Love M. I., Huber W., Anders S. (2014). Moderated estimation of fold change and dispersion for RNA-seq data with DESeq2. *Genome Biology*, 15: 550. Doi: 10.1186/s13059-014-0550-8

Mutukula N., Man Z., Takahashi Y., Martinez F. I., Morales M., Carreon-Guarnizo E, … Izpisua J. C. B. (2021). Generation of RRMS and PPMS specific iPSCs as a platform for modeling multiple sclerosis. *Stem Cell Research,* 53: 1-8. Doi: 10.1016/j.scr.2021.102319

Nuyts A. H., Lee W. P., Bashir-Dar R., Bernemann Z. N., Cools N. (2013). Dendritic cells in multiple sclerosis: key players in the immunopathogenesis, key players for new cellular immunotherapies? *Multiple Sclerosis Journal*, 19 (8), 995-1002. Doi: 10.1177/1352458512473189

Pollier J., Rombauts S., Goossens A. (2013). Analysis of RNA-seq data with TopHat and Cufflinks for genome-wide expression analysis of jasmonate-treated plants and plant cultures. *Methods in Molecular Biology*, 1011: 305-315. Doi: 10.1007/978-1-62703-414-2_24.

Protein atlas. https://www.proteinatlas.org/

Ramesh A., Schubert R. D., Greenfield A. L., Dandekar R., Loudermilk R., Sabatino J., … Wilson M. R. (2020). A pathogenic and clonally expanded B cell transcriptome in active multiple sclerosis. *Proceedings of the National Academy of Sciences*, 117 (37): 22932-22943. Doi: 10.1073/pnas.2008523117.

Schroder M., Melum G. R., Landsverk O. L. B., Bujiko A., Yaqub S., Gran E., … Richter L. (2016). CD1c-Expression by Monocytes - Implications for the Use of Commercial CD1c^{+} Dendritic Cell Isolation Kits. *Plos One*, 11 (6): e0157387. Doi: 10.1371/journal.pone.0157387

Serafini B., Rosicarelli B., Magliozzi R., Stigliano E., Capello E, Mancardi G. L., Aloisi F. (2006). Dendritic cells in multiple sclerosis lesions: maturation stage, myelin uptake, and interaction with proliferating T cells. *Journal of Neuropathology and Experimental Neurology*, 65 (2): 124-141. Doi: 10.1097/01.jnen.0000199572.96472.1c

Shi J., Ikeda K., Maeda Y., Shiagawa K., Ohtsuka A., Yamamura H., Tanimoto M. (2008). Identification of $CD123^+$ myeloid dendritic cells as an early-stage immature subset with strong tumoristatic potential. *Cancer letters*, 270 (1): 19-29. Doi: 10.1016/j.canlet.2008.04.048

Stasiolek M., Bayas A., Kruse N., Wieczarkowiecz A., Toyka K. V., Gold R., Selmaj K. (2006). Impaired maturation and altered regulatory function of plasmacytoid dendritic cells in multiple sclerosis. *Brain*, 129: 1293-1305. Doi:10.1093/brain/awl043

Stephen L., Hauser M. D., Bruce A. C., Cree M. D. (2020). Treatment of Multiple Sclerosis: A Review. *The American Journal of Medicine*, 133 (12): 1380–1390. Doi: 10.1016/j.amjmed.2020.05.049.

Thewissen K., Nuyts A. H., Deckx N., Wijmeersch B. V., Nagels G., D'hooghe M., … Cools N. (2014). Circulating dendritic cells of multiple sclerosis patients are proinflammatory and their frequency is correlated with MS-associated genetic risk factors. *Multiple sclerosis journal*, 20 (5): 548-557. Doi: 10.1177/1352458513505352

Thompson A. J., Baranzini S. E., Geurts J., Hemmer B., Ciccarelli O. (2018). Multiple sclerosis. *The Lancet*, 391 (10130): 1622-1636. Doi: 10.1016/S0140-6736(18)30481-1.

Villani A. C., Satija R., Reynolds G., Sarkizova S., Shekhar K., Fletcher J., … Hacochen N. (2017). Single-cell RNA-seq reveals new types of human blood dendritic cells, monocytes and progenitors. *Science*, 21: 356-387. Doi:10.1126/science.aah4573.

Wang Z., Gerstein M., Snyder M. (2009). RNA-seq: a revolutionary tool for transcriptomics. *Nature Reviews Genetics,* 10 (1): 57-63. Doi: 10.1038/nrg2484.

Xie Z. X., Zhang H. L., Wu X. J., Zhu J., Ma D. H., Jin T. (2015). Role of the immunogenic and tolerogenic subsets of dendritic cells in multiple sclerosis. *Mediator of Inflammation*, 2015: 513295. Doi: 10.1155/2015/513295.